F. Santosa and H. Zhang *Res Math Sci* (2020) 7:15
https://doi.org/10.1007/s40687-020-00211-w

Research in the Mathematical Sciences

RESEARCH

Photonic band gap phenomenon in a metal–dielectric periodic structure

Fadil Santosa[1*] and Hai Zhang[2]

*Correspondence: santosa@umn.edu
[1]School of Mathematics, University of Minnesota, Minneapolis, MN 55455, USA
Full list of author information is available at the end of the article

Abstract

We study the photonic band structure of a metal–dielectric periodic structure. The metallic component is described by the Drude model; therefore, the electric permittivity is frequency dependent, i.e., dispersive. Rather than solving a nonlinear eigenvalue problem for the band structure of the material, we follow a time-dependent formulation described in Raman and Fan (Phys Rev Lett 104:087401, 2010) which leads to a linear eigenvalue problem. At issue is the question of completeness of the eigenfunctions, which is claimed but not proven in Raman and Fan (2010). We establish completeness in one dimension. We further describe the existence of accumulation points in the spectrum that lead to an infinite family of 'zero group velocity' waves. Numerical calculations illustrate some of the main ideas of this work.

Keywords: Photonic band gaps, Spectral theory, Metallic optical material, Bloch waves, Eigenfunction expansions

1 Introduction

The possibility of creating a periodic structure using a combination of metals (e.g., gold) and dielectric (e.g., air) has open novel possibilities for manipulating light. In Scalora et al. [7], the authors studied the possibility of tunable transparent structures using such composites. Investigation of the absorption properties of simple three-dimensional metallic periodic structures with different metals was carried out in El Kady et al. [2]. An approach for creating a wide band gap in a metal–dielectric photonic crystal is discussed in Wu et al. [9].

In [5], Raman and Fan proposed an attractive way of computing the band structure or dispersion curves associated with a metal–dielectric periodic structure. In the work, they used the Drude model in the metal portion of the medium, which means that the time-harmonic electromagnetic (EM) field, which satisfies Maxwell's equation, has an electric permittivity which is frequency dependent. Therefore, solving for the dispersion relation, i.e., the dependence of frequency on quasi-momentum, leads to a nonlinear eigenvalue problem. Since methods for solving nonlinear eigenvalue problems are not as well developed as those for linear eigenvalue problems, this presents a computational challenge.

It is possible to write the equations governing the EM field in metal in the time domain as pointed out in [5]. This leads to a system involving two additional dependent variables—the polarization and the polarization velocity. We describe this in the next section. The advantage of considering this enlarged system is that the eigenvalue problem associated with computing dispersion relation is *linear*.

While it is clear how one can now proceed to use an eigenvalue problem solver to calculate the dispersion curves numerically, the problem formulation introduces a mathematical issue which is not fully addressed in [5]. The issue arises because the part of the operator corresponding to the polarization fields is a multiplication operator whose inverse is not compact. The coupling of this operator with the differential operators opens the possibility of a continuous spectrum, see, e.g., Hislop and Sigal [4].

Our work resolves the aforementioned issue with regard to the operators involved. Standard techniques for showing completeness of the eigenfunctions for elliptic operators do not apply. For the case of one-dimensional periodic structure, it is possible to derive an expression for the eigenvalues associated with the operator. Using the Weyl's criterion argument, we can establish completeness.

The paper is organized in the following way: We first re-introduce the time domain formulation described in [5] in Sect. 2. In Sect. 3, we specialize the one-dimensional problem and investigate the problem in detail. We first study the eigenvalue problem associated with the periodic structure. Since it is somewhat simple, we are able to give a precise characterization of all the eigenvalues for a given momentum. This is followed by a spectral analysis of the associated operator and a proof of completeness of eigenfunctions. We further discretize the system and produced numerical examples. The properties of the dispersion curves as well as the eigenfunctions are examined. Section 4 is a discussion which summarizes the work and describes possible research directions.

We finally note that an alternate computational strategy for computing band gaps in general frequency-dependent material has been proposed in Toader and John [8]. The method involves 'lifting' the problem to a higher dimension wherein the associated eigenvalue problem is easy to solve. The desired dispersion relation is then extracted by intersection with appropriately chosen cutting surfaces.

2 Time domain formulation

Consider a metal–dielectric periodic structure. Let $\Omega \in \mathbb{R}^3$ be a periodic cell made up of disjoint sets Ω_{m} and Ω_{d}. In Ω_{m}, the metal, EM fields satisfy

$$\mu \dot{\mathbf{H}} = -\nabla \times \mathbf{E}, \tag{1}$$

$$\epsilon \dot{\mathbf{E}} = \nabla \times \mathbf{H} - \mathbf{V}, \tag{2}$$

$$\dot{\mathbf{P}} = \mathbf{V}, \tag{3}$$

$$\dot{\mathbf{V}} = \omega_{\mathrm{p}}^2 \epsilon \mathbf{E} - \omega_0^2 \mathbf{P}. \tag{4}$$

Here, $\mathbf{E}$ and $\mathbf{H}$ are the electric and magnetic fields, while $\mathbf{P}$ and $\mathbf{V}$ are the polarization and polarization velocity fields. The electric permittivity and magnetic permeability of air are ϵ and μ. The dots over the variables denote time derivative. The parameter ω_{p} is the plasma frequency, and ω_0 is the characteristic frequency of the polarization field. When $\mathbf{P}$ and $\mathbf{V}$ are eliminated from the equations, we would arrive at an EM field satisfying an

apparent electric permittivity given by

$$\overline{\epsilon}(\omega) = \epsilon\left(1 + \frac{\omega_{\mathrm{p}}^2}{\omega_0^2 - \omega^2}\right). \tag{5}$$

We note here that unlike in [5], we are considering the undamped system. In the dielectric, Ω_{d}, we have Maxwell's equation, obtained by setting **P** and **V** to zero in (1)–(2).

Consider a periodic structure consisting of cubes of size p. Let Ω_{m} be a ball of diameter less than p, and it is centered in the cube; Ω_{d} is the surrounding dielectric. In the metal, (1)–(4) apply, whereas in the dielectric, there are no **P** or **V** fields. We require that the tangential components of **H** and **E** be continuous across the metal–dielectric interface

$$[\![\mathbf{H} \times \mathbf{n}]\!] = [\![\mathbf{V} \times \mathbf{n}]\!] = 0, \tag{6}$$

where **n** is the normal to Ω_{m} and $[\![\mathbf{u}]\!]$ is the jump of **u** across the boundary of Ω_{m}.

Now, we seek time-harmonic solution of the form $\mathbf{H}e^{i\omega t}$, etc. We continue to use **H**, etc., to describe the frequency-dependent fields in a slight abuse of notation. Therefore in Ω_{m}, we have

$$\omega\begin{bmatrix}\mathbf{H}\\ \mathbf{E}\\ \mathbf{P}\\ \mathbf{V}\end{bmatrix} = \begin{bmatrix} 0 & \frac{i}{\mu}\nabla\times & 0 & 0\\ -\frac{i}{\epsilon}\nabla\times & 0 & 0 & \frac{i}{\epsilon}\\ 0 & 0 & 0 & -i\\ 0 & -i\omega_{\mathrm{p}}^2\epsilon & i\omega_0^2 & 0\end{bmatrix}\begin{bmatrix}\mathbf{H}\\ \mathbf{E}\\ \mathbf{P}\\ \mathbf{V}\end{bmatrix}. \tag{7}$$

In Ω_{d}, we have

$$\omega\begin{bmatrix}\mathbf{H}\\ \mathbf{E}\end{bmatrix} = \begin{bmatrix} 0 & \frac{i}{\mu}\nabla\times\\ -\frac{i}{\epsilon}\nabla\times & 0\end{bmatrix}\begin{bmatrix}\mathbf{H}\\ \mathbf{E}\end{bmatrix}. \tag{8}$$

The quasi-periodic boundary conditions for **H** and **E** are

$$\begin{aligned}\mathbf{H}(\mathbf{x} + p\mathbf{e}_j) &= \mathbf{H}(\mathbf{x})e^{i\mathbf{k}\cdot\mathbf{e}_j p},\\ \mathbf{E}(\mathbf{x} + p\mathbf{e}_j) &= \mathbf{E}(\mathbf{x})e^{i\mathbf{k}\cdot\mathbf{e}_j p}, \quad j = 1, 2, 3,\end{aligned} \tag{9}$$

where $\mathbf{e}_j$ is the unit vector in the x_j direction, and **k** is the quasi-momentum. Equations (7), (8), and (9), together with the continuity conditions on the tangential components of **H** and **E** in (20), represent the eigenvalue problem that we must solve for every **k**. We note that this is a linear eigenvalue problem.

Following [5], we define a diagonal matrix

$$\mathcal{A} = \mathrm{diag}\left(\mu, \epsilon, \frac{\omega_0^2}{\omega_{\mathrm{p}}^2\epsilon}, \frac{1}{\omega_{\mathrm{p}}^2\epsilon}\right),$$

and operator matrix

$$\mathcal{B} = \begin{bmatrix} 0 & i\nabla\times & 0 & 0\\ -i\nabla\times & 0 & 0 & i\\ 0 & 0 & 0 & -i\frac{\omega_0^2}{\omega_{\mathrm{p}}^2\epsilon}\\ 0 & -i & i\frac{\omega_0^2}{\omega_{\mathrm{p}}^2\epsilon} & 0\end{bmatrix}.$$

It should be noted that viewing $\mathcal{B}$ as a matrix, it is Hermitian in the sense that its elements satisfy $b_{kl} = \overline{b_{kl}}$, where overline indicates complex conjugation. Letting $\mathbf{z} = [\mathbf{H}, \mathbf{E}, \mathbf{P}, \mathbf{V}]^T$ and $\mathbf{y} = \mathcal{A}^{\frac{1}{2}}\mathbf{z}$, the system (7) can be rewritten as

$$\omega \mathbf{y} = \mathcal{C}\mathbf{y}, \tag{10}$$

where

$$\mathcal{C} = \mathcal{A}^{-\frac{1}{2}}\mathcal{B}\mathcal{A}^{-\frac{1}{2}} = \begin{bmatrix} 0 & i\frac{1}{\sqrt{\epsilon\mu}}\nabla\times & 0 & 0 \\ -i\frac{1}{\sqrt{\epsilon\mu}}\nabla\times & 0 & 0 & i\omega_{\mathrm{P}} \\ 0 & 0 & 0 & -i\omega_0 \\ 0 & -i\omega_{\mathrm{P}} & i\omega_0 & 0 \end{bmatrix}$$

is Hermitian when viewed as a matrix.

As pointed out in [5], it is possible to model the fields in the dielectric by setting $\omega_0 \to \infty$ and $\omega_{\mathrm{P}} \to 0$ in the Drude model. This fact allows them to focus on the operator $\mathcal{C}$ for the metal–dielectric structure. In this work, we continue to use different equations in the two media. The operator $\mathcal{C}$ as in (10) is valid only in the metal. In the dielectric, with $\mathbf{z}' = [\mathbf{H}, \mathbf{E}]$, and $\mathcal{A}' = \mathrm{diag}(\mu, \epsilon)$, so $\mathbf{y}' = \mathcal{A}'^{\frac{1}{2}}\mathbf{z}'$. We have

$$\omega \mathbf{y}' = \mathcal{C}'\mathbf{y}', \tag{11}$$

where

$$\mathcal{C}' = \mathcal{A}'^{-\frac{1}{2}} \begin{bmatrix} 0 & i\nabla\times \\ -i\nabla\times & 0 \end{bmatrix} \mathcal{A}'^{-\frac{1}{2}}.$$

In [5], the authors argued that since $\mathcal{C}$ is Hermitian (presumably for any nonzero ω_0 and ω_{P}), eigenvalue problem (10) with the quasi-periodic boundary conditions (9) should lead to eigenfunctions $\mathbf{y}_m$ which are orthogonal for every $\mathbf{k}$. This can be shown using an integrations-by-parts argument. What they claim next is that the eigenfunctions form a complete set. While the authors were not specific in their meaning of completeness, we can surmise that they mean given a $\mathbf{k}$, the set of eigenfunctions satisfying (11), $\{\mathbf{y}_1, \mathbf{y}_2, \ldots\}$, spans $L^2(\Omega)$. This statement is not proven in the paper. Instead, the authors cited a result in Courant and Hilbert [1]. In fact, the result in [1] covers the classical case of eigenvalue problems for a differential operator whose inverse is compact. The present case is not covered by the classical theorem cited. The operator $\mathcal{C}$ actually couples a differential operator, whose inverse is compact, with a multiplication operator, whose inverse is unbounded. Consequently, the inverse of $\mathcal{C}$ is *not* a compact operator in $H^1(\Omega)$.

We take a step back and observe that in fact there are two fields—$\mathbf{y}$ in the metal and $\mathbf{y}'$ in the dielectric. They satisfy (10) and (11), respectively. They are coupled at the metal–dielectric interface where the tangential components of the first two entries of $\mathbf{y}$ match with the tangential components of $\mathbf{y}'$. Moreover, on the boundaries of the periodic cell, quasi-periodic boundary conditions apply to the first two components of $\mathbf{y}$ (as in (9)). Let $(\mathbf{y}_m, \mathbf{y}'_m)$ and $(\mathbf{y}_n, \mathbf{y}'_n)$ be eigenfunctions of (10) and (11) for eigenvalues $\Omega_{\mathrm{m}} \neq \omega_n$. Then by integration-by-parts, we have

$$\int_{\Omega_{\mathrm{m}}} \mathbf{y}_m \cdot \overline{\mathbf{y}_n}\, \mathrm{d}x + \int_{\Omega_{\mathrm{d}}} \mathbf{y}'_m \cdot \overline{\mathbf{y}'_n}\, \mathrm{d}x = \delta_{mn}. \tag{12}$$

On the other hand, completeness is not as obvious. However, in the subsequent we will show that in one dimension, completeness is a consequence of the fact that the continuous spectrum is empty.

3 One-dimensional problem

We start with the full system in [5] which is in the Hermitian form

$$\mathcal{C} = \begin{bmatrix} 0 & i\frac{1}{\sqrt{\epsilon\mu}}\nabla\times & 0 & 0 \\ -i\frac{1}{\sqrt{\epsilon\mu}}\nabla\times & 0 & 0 & i\omega_{\mathrm{P}} \\ 0 & 0 & 0 & -i\omega_0 \\ 0 & -i\omega_{\mathrm{P}} & i\omega_0 & 0 \end{bmatrix}$$

For the one-dimensional model we consider, we have

$$\mathbf{E} = (0, E, 0),\ \mathbf{H} = (0, 0, H),\ \mathbf{P} = (0, P, 0),\ \mathbf{V} = (0, V, 0),$$

where the scalar functions E, H, P, V depend only on the variable x_1. To simplify our presentation, we shall henceforth drop the subscript from x_1. We set the period of the structure to be unity and focus on reference cell $[0, 1]$. We also set $\epsilon = \mu = 1$. The metal extends over the interval $[0, \theta]$, with $0 < \theta < 1$. The parameter θ is the volume fraction of metal. The eigenvalue problem reduces to

$$\omega \begin{bmatrix} H \\ E \\ P \\ V \end{bmatrix} = \begin{bmatrix} 0 & iD_x & 0 & 0 \\ iD_x & 0 & 0 & i\omega_{\mathrm{p}} \\ 0 & 0 & 0 & -i\omega_0 \\ 0 & -i\omega_{\mathrm{p}} & i\omega_0 & 0 \end{bmatrix} \begin{bmatrix} H \\ E \\ P \\ V \end{bmatrix}, \quad 0 < x < \theta, \tag{13}$$

and

$$\omega \begin{bmatrix} H \\ E \end{bmatrix} = \begin{bmatrix} 0 & iD_x \\ iD_x & 0 \end{bmatrix} \begin{bmatrix} H \\ E \end{bmatrix}, \quad \theta < x < 1, \tag{14}$$

with quasi-periodic boundary conditions

$$H(x+1) = H(x)e^{ik}, \quad E(x+1) = E(x)e^{ik}, \tag{15}$$

and continuity conditions

$$[H]_{x=\theta} = 0, \quad [E]_{x=\theta} = 0. \tag{16}$$

Equations (13)–(14), along with the boundary conditions, should yield, for each k, eigenvalues $\omega_n(k)$. Associated with an eigenvalue is the solution (H_n, E_n, P_n, V_n). We view the solutions as eigenvectors. These eigenvectors are orthogonal under the following inner product

$$\int_0^\theta \frac{1}{2}(E_m\overline{E_n} + H_m\overline{H_n}) + \frac{1}{2\omega_{\mathrm{p}}^2}(V_m\overline{V_n} + \omega_E^2 P_m\overline{P_n})\mathrm{d}x + \int_\theta^1 \frac{1}{2}(E_m\overline{E_n} + H_m\overline{H_n})\mathrm{d}x = \delta_{mn}.$$

This orthogonality condition follows from (12) but is given in terms of the native variables (H, E, P, V).

3.1 Eigenvalue problem

We proceed by solving the eigenvalue problem in (13)–(16). To do this, we eliminate P and V in (13) and deal only with the variable E. It is shown to satisfy

$$E'' + \sigma^2\omega^2 E = 0, \quad 0 < x < \theta. \tag{17}$$

Here, σ is the square root of the frequency-dependent permittivity described by Drude's model

$$\sigma^2 = 1 + \frac{\omega_{\mathrm{P}}^2}{\omega_0^2 - \omega^2}.$$

Equation (14) reduces to

$$E'' + \omega^2 E = 0, \quad \theta < x < 1. \tag{18}$$

The quasi-periodic conditions now apply to E and its derivative:

$$E(1) = E(0)e^{ik}, \quad E'(1) = E'(0)e^{ik}. \tag{19}$$

Continuity conditions now read

$$[E]_{x=\theta} = 0, \quad [E']_{x=\theta} = 0. \tag{20}$$

It is important to point out the sign change in σ^2:

$$\sigma^2 \geq 0, \quad 0 \leq \omega < \omega_0 \ \text{ and } \ \omega \geq \sqrt{\omega_0^2 + \omega_{\mathrm{P}}^2},$$
$$\sigma^2 < 0, \quad \omega_0 < \omega < \sqrt{\omega_0^2 + \omega_{\mathrm{P}}^2}.$$

We solve the eigenvalue problem by assuming a solution of the form

$$E(x) = \begin{cases} A\cos(\sigma\omega x) + B\sin(\sigma\omega x), & 0 < x < \theta \\ C\cos(\omega(1-x)) + D\sin(\omega(1-x)), & \theta < x < 1 \end{cases}. \tag{21}$$

From the quasi-periodicity condition (19), we get

$$C = Ae^{ik}, \quad D = -\sigma Be^{ik}.$$

Continuity conditions (20) lead to

$$A\cos(\sigma\omega\theta) + B\sin(\sigma\omega\theta) = C\cos(\omega(1-\theta)) + D\sin(\omega(1-\theta)),$$
$$\sigma[-A\sin(\sigma\omega\theta) + B\cos(\sigma\omega\theta)] = C\sin(\omega(1-\theta)) - D\cos(\omega(1-\theta)).$$

Substituting C and D in the two equations, we get

$$A(\cos(\sigma\omega\theta) - e^{ik}\cos(\omega(1-\theta))) + B(\sin(\sigma\omega\theta) + e^{ik}\sigma\sin(\omega(1-\theta))) = 0,$$
$$-A(\sigma\sin(\sigma\omega\theta) + e^{ik}\sin(\omega(1-\theta))) + B\sigma(\cos(\sigma\omega\theta) - e^{ik}\cos(\omega(1-\theta))) = 0.$$

The dispersion relation is obtained by requiring that the determinant associated with the linear system be zero, which after some simplification yields

$$2\cos k = 2\cos(\sigma\omega\theta)\cos(\omega(1-\theta)) - \frac{1+\sigma^2}{\sigma}\sin(\sigma\omega\theta)\sin(\omega(1-\theta)). \tag{22}$$

Equation (22) is the nonlinear eigenvalue problem associated with the system. We do not use it for computational purposes. However, the equation does reveal certain properties of the roots $\{\omega_n(k)\}$:

- There are an infinitely many roots for each k.
- There are two sets of roots separated by whether $\omega_n(k)$ are less than or greater than ω_0.
- The roots $\omega_n(k) < \omega_0$ have accumulation points at ω_0.
- The roots $\omega_n(k) > \omega_0$ approach ∞.

These observations can be explained by examining σ as a function of ω. Notice that

$$\sigma \to 1 \quad \text{as} \quad \omega \to \infty.$$

Therefore for large ω, (22) simplifies to

$$2\cos k \approx 2\cos(\omega).$$

This means $\omega_n(k) \to k + 2n\pi$ for large n.

For $(\omega_0 - \omega)$ small and positive, σ is large; therefore, (22) is approximately

$$2\cos k = 2\cos(\sigma\omega\theta)\cos(\omega_0(1-\theta)) - \sigma\sin(\sigma\omega(1-\theta))\sin(\omega_0(1-\theta)).$$

Both terms on the right-hand side oscillate faster and faster and grow in amplitude as ω approaches ω_0, equating with the value on the left-hand side more and more often. This accounts for the accumulation phenomenon at ω_0.

We note that the accumulation point ω_0 exists for any k and for any volume fraction θ. As we shall see in Sect. 3.3, this leads to an interesting feature in the dispersion curves. We summarize the above observations into the following proposition.

Proposition 1 *For each k, the eigenvalue problem* (13)–(16) *has an essential spectrum* ω_0 *as the accumulation point of its eigenvalues [3].*

So far, we have shown that all the eigenvalues of the eigenvalue problem (13)–(16) satisfy Eq. (22) and that there are infinitely many of them. Their corresponding eigenfunctions can be calculated accordingly. A natural question to ask is: For each k, do these eigenfunctions form a complete bases? This is not obvious from our calculation. We shall show that the answer is yes in the next section by using Weyl's criterion.

3.2 Weyl's criterion argument

In the section, we aim to prove the completeness of eigenfunctions for the eigenvalue problem (13)–(16) . The idea is to analyze the spectrum of the associated unbounded operator. A key step is to use the Weyl's criterion to determine its essential spectrum and show that the essential spectrum consists of only one point. We refer reader to chapter VIII in Reed and Simon [6] for an excellent treatment of spectral theory of unbounded self-adjoint operators that are used in our arguments.

To start with, we define the Hilbert space

$$\mathbf{X} = L^2(0,1) \times L^2(0,1) \times L^2(0,\theta) \times L^2(0,\theta).$$

Then, the operator $\mathcal{C}$ reduces to the following unbounded operator C in $\mathbf{X}$:

$$C \begin{bmatrix} H \\ E \\ P \\ V \end{bmatrix} = \begin{bmatrix} 0 & iD_x & 0 & 0 \\ iD_x & 0 & 0 & i\omega_{\mathrm{p}} \\ 0 & 0 & 0 & -i\omega_0 \\ 0 & -i\omega_{\mathrm{p}} & i\omega_0 & 0 \end{bmatrix} \begin{bmatrix} H \\ E \\ P \\ V \end{bmatrix} = \begin{bmatrix} iE' \\ iH' + iV \\ -i\omega_0 V \\ -iE + i\omega_0 P \end{bmatrix}.$$

For each $k \in [0, 2\pi)$, we define

$$\mathbf{X}_k = \{(H,E,P,V)^T \in \mathbf{X} : H, E \in H^1(0,1), \\ H(x+1) = H(x)e^{ik},\ E(x+1) = E(x)e^{ik}\}.$$

It is clear that the boundary conditions (15)–(16) are encoded in the definition of the space $\mathbf{X}_k$ and the eigenvalues of the eigenvalue problem (13)–(16) are equivalent to the point spectrum of the operator C with domain $D(C) = \mathbf{X}_k$.

Lemma 1 *The operator C is unbounded and is self-adjoint in the Hilbert space $\boldsymbol{X}$ with domain $D(C) = \boldsymbol{X}_k$.*

Proof It is straightforward to check that C is symmetric in the sense that

$$(Cf, g) = (f, Cg), \quad \text{for all } f, g \in D(C).$$

To show the self-adjointness, we need only to show that $\mathrm{Ran}(C \pm iI) = \mathbf{X}_k$ (see Chapter VIII in [6]). Let $S = (S_1, S_2, S_3, S_4)^T \in \mathbf{X}_k$, we will try to solve $(C - \lambda I)(H, E, P, V)^T = S$, with $\lambda = i$. More precisely, consider

$$iE' - \lambda H = S_1, \tag{23}$$
$$iH' + iV - \lambda E = S_2, \tag{24}$$
$$-i\omega_0 V - \lambda P = S_3, \tag{25}$$
$$-iE + i\omega_0 P - \lambda V = S_4. \tag{26}$$

We use (25)–(26) to solve for P and V in terms of E, S_3, and S_4. After inverting a 2-by-2 linear system, we get

$$V = \frac{i\omega_0 S_3 + i\lambda E + \lambda S_4}{\omega_0^2 - \lambda^2}. \tag{27}$$

Next, we take the derivative of (23) and solve for E''

$$E'' = -iS_1' - i\lambda H'.$$

Substituting this in H' from (24) in the above, we get

$$E'' - \lambda^2 E + i\lambda V \chi_\theta = -iS_1' - \lambda S_2,$$

where χ_θ is the characteristic function of the interval $[0, \theta]$. Finally, we substitute V in (27) to get

$$E'' + \lambda^2 \left(1 + \frac{\chi_\theta}{\omega_0^2 - \lambda^2}\right) E = -iS_1' - \lambda S_2 + \frac{i\lambda}{\omega_0^2 - \lambda^2}(i\omega_0 S_3 + \lambda S_4)\chi_\theta. \tag{28}$$

With the given quasi-periodic boundary condition, we can show that Eq. (28) for E is uniquely solvable for $\lambda = i$. After we get E, we can derive P, V, and H subsequently. This shows that $\mathrm{Ran}(C - iI) = \mathbf{X}_k$. Similarly, one can show that $\mathrm{Ran}(C + i) = \mathbf{X}_k$. Therefore, C is self-adjoint. □

We now use the Weyl's criterion (see Sigal and Hislop [4], Chapter 7) to argue that there is only one essential spectrum of C. We first recall the definition of Weyl's sequence.

Definition 1 A sequence $\{u_n\}$ is called a Weyl sequence for C and λ if there exists $\{u_n\} \subset D(C)$ such that $\|u_n\| = 1$, $u_n \xrightarrow{w} 0$ and $(C - \lambda)u_n \xrightarrow{s} 0$.

Here, by $\xrightarrow{s}$ and $\xrightarrow{w}$ we mean strong and weak convergences of sequences.

Theorem 1 (Weyl's criterion) *Let C be self-adjoint. Then, $\lambda \in \sigma_{\mathrm{ess}}(C)$ if and only if there exists a Weyl sequence for C and λ.*

Theorem 2 *The essential spectrum of the operator C consists of only one point which is ω_0.*

Proof We have shown that ω_0 is an essential spectrum of C (see Proposition 1). We need to only show that it is the only one. We prove this by contradiction. Assume that $\lambda \neq \omega_0$ is an essential spectrum of C. We first consider the following system of equations:

$$(C - \lambda I)U = S,$$

where $U = (H, E, P, V)^T$, $S = (S_1, S_2, S_3, S_4)$ and all the variables depend on x only. The equations are already given in (23)–(26). From (28), we can conclude that if S_j for $j = 1, 2, 3, 4$ and E are bounded in $L^2(0, 1)$, then E is bounded in $H^1(0, 1)$.

Now, if λ is an essential spectrum, by the Weyl criterion, there exists a Weyl sequence $U_n = (H_n, E_n, V_n, P_n) \in \mathbf{X}$ such that $\|U_n\|_{\mathbf{X}} = 1$ and $U_n \xrightarrow{w} 0$ in $\mathbf{X}$. Moreover, $(C - \lambda I)U_n = S^{(n)}$ with $\|S^{(n)}\|_{\mathbf{X}} \xrightarrow{s} 0$.

By (28), we can derive that $\|E_n\|_{H^1(0,1)}$ is uniformly bounded. As a result, we can extract a subsequence, still denoted by E_n such that $E_n \to E^*$ weakly in $H^1(0, 1)$ for some function E^* in $H^1(0, 1)$. But $E_n \to 0$ weakly in $L^2(0, 1)$. By the uniqueness of weak limit, we can conclude that $E^* = 0$ and therefore $E_n \to 0$ weakly in $H^1(0, 1)$. Using the fact that $H^1(0, 1)$ is compactly embedded in $L^2(0, 1)$, we see that one can further extract a subsequence of E_n, say E_{n_j} such that $E_{n_j} \to 0$ in $L^2(0, 1)$. From (27), we conclude that $V_{n_j} \to 0$ in L^2 also. The same conclusion can be drawn about P_{n_j} from (25). Finally, consider (24) which we rewrite as

$$H_{n_j}' = -iS_{n_j} - V_{n_j} - i\lambda E_{n_j}.$$

We have shown that the right-hand side tends to 0 in $L^2(0, 1)$. Therefore, $H_{n_j} \to 0$ strongly in L^2. However, H_{n_j} is uniformly bounded in $L^2(0, 1)$. We see that H_{n_j} is uniformly bounded in $H^1(0, 1)$. Similar to the argument for E_n, we can further extract a subsequence, still

denoted by H_{n_j}, such that $H_{n_j} \to 0$ strongly in $L^2(0,1)$. Combining all these results, we see that

$$U_{n_j} \to 0, \quad \text{strongly in } \mathbf{X},$$

which contradicts to the fact that $\|U_n\|_{\mathbf{X}} = 1$. This contradiction shows that $\lambda \neq \omega_0$ is not an essential spectrum of C. This completes the proof of the theorem. □

As a consequence, we obtain the following main result on the spectrum of the unbounded self-adjoint operator C. In particular, the result establishes completeness of the eigenfunctions for each quasi-momentum k.

Theorem 3 *For each quasi-momentum $k \in [0, 2\pi)$, the following statements hold for the operator C in $\boldsymbol{X}$ with $D(C) = \boldsymbol{X}_k$:*

1. *The continuous spectrum $\sigma_{\text{cont}}(C)$ is empty;*
2. *The spectrum $\sigma(C)$ equals to $\overline{\sigma_{pp}(C)}$, where $\sigma_{pp}(C)$ is the set of point spectrum of C. Moreover, $\sigma_{pp}(C)$ has only one accumulation point which is ω_0;*
3. *The set of normalized eigenfunctions of C form a complete orthonormal basis for $\boldsymbol{X}_k$.*

3.3 Numerics

In this section, we discretize (13)–(14) and solve for the dispersion curves $\omega_n(k)$ and the associated eigenfunctions. In the metal, the state variable is $\mathbf{y} = [H, E, \frac{\omega_0}{\omega_{\text{P}}} P, \frac{1}{\omega_{\text{P}}} V]^T$ and the equation is

$$\omega \mathbf{y} = C\mathbf{y}, \tag{29}$$

where

$$C = \begin{bmatrix} 0 & iD_x & 0 & 0 \\ iD_x & 0 & 0 & i\omega_{\text{P}} \\ 0 & 0 & 0 & -i\omega_0 \\ 0 & -i\omega_{\text{P}} & i\omega_0 & 0 \end{bmatrix}.$$

In the dielectric, the state variable is $\mathbf{y}' = [H, E]^T$ and the equation is

$$\omega \mathbf{y}' = C'\mathbf{y}, \tag{30}$$

where

$$C' = \begin{bmatrix} 0 & iD_x \\ iD_x & 0 \end{bmatrix}.$$

Continuity conditions are

$$[H]_\theta = [E]_\theta.$$

We also have the quasi-periodicity condition

$$H(1) = H(0)e^{ik}, \quad E(1) = E(0)e^{ik}.$$

After rewriting the solution to take the form, we get

$$\mathbf{y} = \mathbf{w}e^{ikx}, \quad \mathbf{y}' = \mathbf{w}'e^{ikx},$$

where now both $\mathbf{w}$ and $\mathbf{w}'$ are unit periodic.

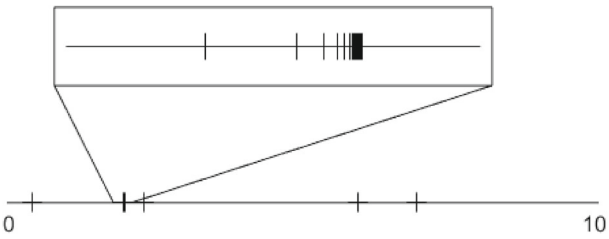

Fig. 1 The spectrum of the Bloch solution for volume fraction $\theta = 0.3$ and wave number $k = 0.5$. There are two accumulation points, at ω_0 and at infinity. This figure highlights the accumulation at ω_0 from the left

We use a staggered grid discretization (Yee scheme [10]) on the periodic functions. The interval $[0, 1]$ is divided into n segments of width $h = 1/n$, with whole grid points

$$x_1 = 0, x_2 = h, x_3 = 2h, \ldots, x_{n+1} = nh,$$

and half grid points

$$x_{1/2} = -h/2, x_{3/2} = h/2, x_{5/2} = 3h/2, \ldots, x_{n+1/2} = (n - 1/2)h.$$

The variable $w_{1,j}$ is defined on x_j, for $j = 1, \ldots, n$ with $w_{1,1} = w_{1,n+1}$. The variable $w_{2,j+1/2}$ is defined on $x_{j+1/2}$, for $j = 0, \ldots, n$, with $w_{2,1/2} = w_{2,n+1/2}$. Choose $\theta = (m-1)h$ for some $m < n$, and we have $w_{3,j+1/2}$ and $w_{4,j+1/2}$ defined only for $j = 1, \ldots, m - 1$. Continuity of H and E across the metal–dielectric interface implies that

$$w_{2,m-1/2} = w_{2,m+1/2},$$

while the discretization forces w_1 are continuous. Now, it is just a matter of writing a matrix eigenvalue problem for the vector

$$\mathbf{w} = [w_{1,1}, \ldots w_{1,n}, w_{2,3/2}, \ldots, w_{2,n+1/2}, w_{3,3/2}, \ldots, w_{3,m-1/2}, w_{4/2}, \ldots, w_{4,m-1/2}]^T,$$

to represent the discrete version of (29)–(30), details of which we omit.

We note here that our discretization correctly couples the metal to the dielectric by eliminating the P and V fields in the dielectric. In [5], the coupling is approximated by setting $\omega_0 = 0$ in the metal and setting ω_0 to a large number and ω_P to a small number.

In the numerical calculations that follow, we set $n = 200$, $\omega_0 = 2$, and $\omega_P = 2.4$. We will vary θ (more precisely m) to understand the effect of the volume fraction on the dispersion curves. The Bloch momentum wave number k is in the interval $[0, \pi]$. We will consider only positive $\omega_i(k)$.

The first calculation illustrates the nature of the spectrum. With $\theta = 0.3$ and $k = 0.5$, we look at the eigenvalues $\omega_i(k)$ lying in the interval $[0, 10]$. This is shown in Fig. 1 where we show the spectrum laid out on the horizontal interval and provide a blowup near ω_0 where there is an accumulation of eigenvalues to the left.

Next, we look at the Bloch spectrum for the same volume fraction. This is shown in Fig. 2. One can easily recognize the presence of band gaps. The shaded region corresponds to frequencies ω for which the metallic segment has a negative permittivity. Notice the 'pile up' of horizontal dispersion curves near $\omega = \omega_0$. This is the result of the accumulation phenomenon we described earlier (Fig. 3). The modes corresponding to these dispersion curves have zero group velocity, much more akin to standing waves with energy concentrated in the metallic regions (Fig. 5C).

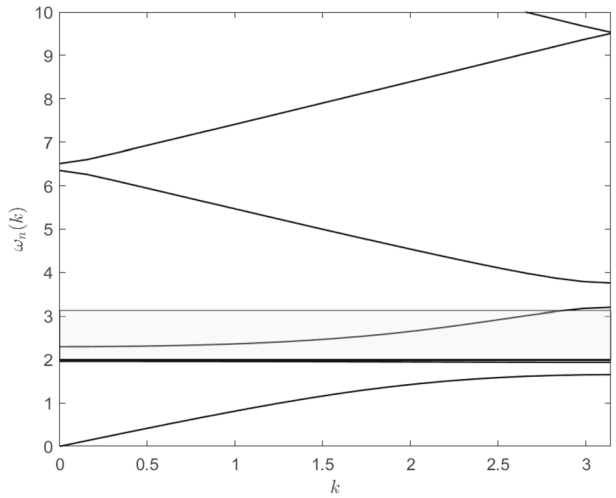

Fig. 2 The Bloch spectrum for $\theta = 0.3$. The shaded region corresponds to values of ω for which the metallic segment has a negative permittivity. Notice the 'pile up' of horizontal dispersion curves just under $\omega = \omega_0$. This is the result of the accumulation phenomenon

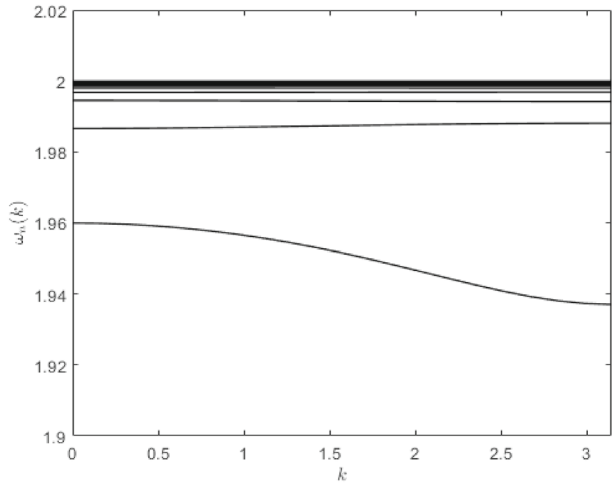

Fig. 3 Blowup of the spectrum in Fig. 2 near $\omega = 2$ highlighting the pile up

We can learn more by examining the eigenfunctions associated with these dispersion curves. We will fix $k = 0.5$ and look at the fields corresponding to H and P. For $i = 1$, that is, the lowest of the branches $\omega_i(k)$, the eigenfunctions have nearly constant amplitude. This is shown in Fig. 4. Note that $P(x)$ is defined only for the metallic section. While the amplitude is nearly constant, the real and imaginary parts are oscillatory. Therefore, these are propagating modes.

For i corresponding to an eigenvalue that is close to the accumulation point, in this case $\omega_i(0.5) = 1.9996$, the eigenfunctions are concentrated in the metallic region as shown in Fig. 5. The group velocity for this mode is nearly zero. These therefore are nonpropagating and are similar to standing waves.

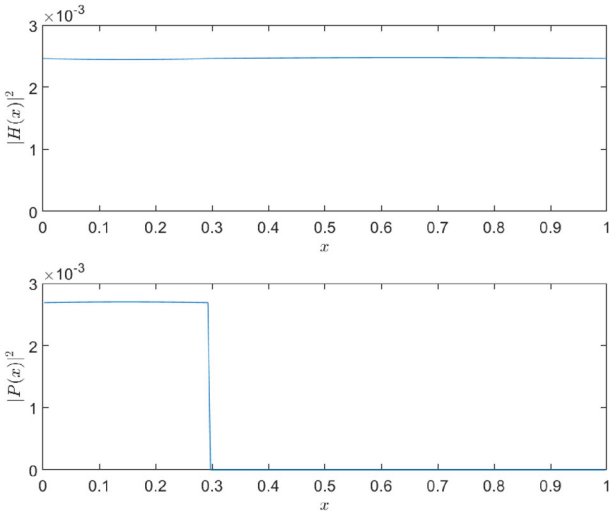

Fig. 4 The amplitude of the eigenfunctions H and P for $\omega_1(0.5)$. Note that the P field only exists in the metal. While the amplitudes are nearly constant, the real and the imaginary parts are oscillatory, corresponding to modes that propagate

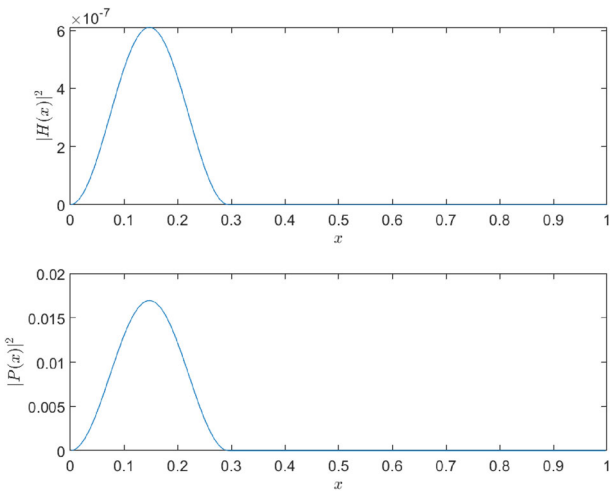

Fig. 5 The amplitude of the eigenfunctions H and P for $\omega_n(0.5)$ near the accumulation point $\omega = \omega_0$. These modes have energy concentrated in the metal regions and are nonpropagating since the group velocity is nearly zero

Finally, when we pick i so that $\omega_i(0.5)$ is in the shaded region (where permittivity in the metal is negative), the eigenfunction for H peaks toward the boundaries between metal and dielectric. A similar phenomenon could be seen in the P field. This is shown in Fig. 6. It should be noted that again the slope of the dispersion curve is nearly zero; therefore, these modes are also nonpropagating.

In the final study, we examine the dependence of the Bloch spectrum on the volume fraction θ. Shown in Fig. 7 are the dispersion curves for $\theta = 0.3$ (L), $\theta = 0.6$ (C), and $\theta = 0.8$ (R). We see that gaps can expand and shrink depending on θ.

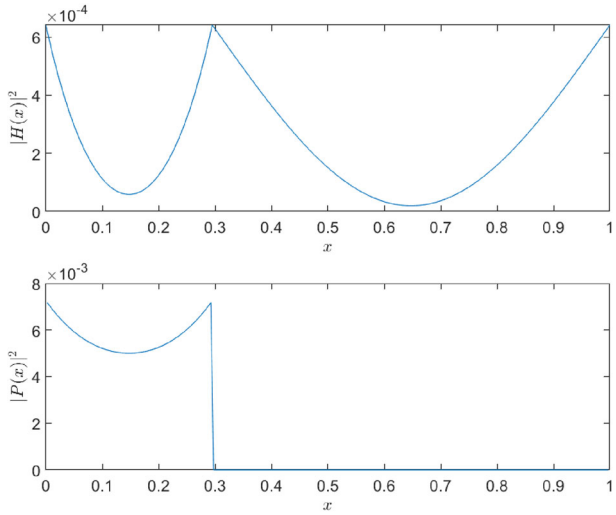

Fig. 6 The amplitude of the eigenfunctions H and P for $\omega_n(0.5)$ in the shaded region where the metal has negative permittivity. Note the concentration of energy at the metal–dielectric interfaces. With group velocity near zero, these are nonpropagating modes

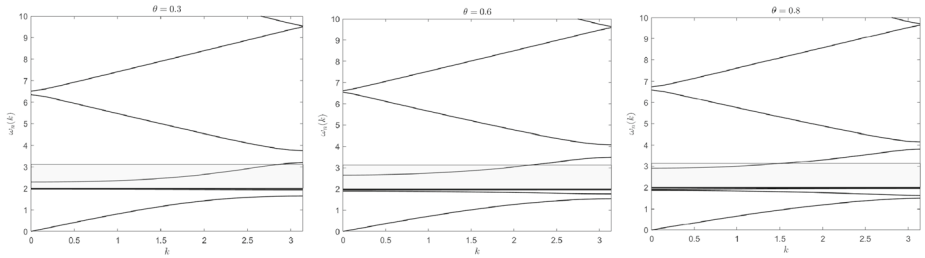

Fig. 7 The dispersion curves for different values of volume fraction θ. Notice that the gaps can expand or shrink as θ is varied

4 Discussion

In this paper, we investigated the spectral properties of dispersive metal–dielectric periodic structure. Such a problem naturally leads to a nonlinear eigenvalue problem. Following [5], we reformulate the problem into a linear eigenvalue problem by introducing additional variables. Using Weyl's criterion, we showed that in one dimension the associated self-adjoint operator has one, and only one, essential spectrum at the characteristic frequency of the polarization field ω_0 in the metal. We resolved the issue of the completeness of the eigenfunctions for this particular case. Our study also explains the phenomenon of pile up of the dispersion curves near the singular frequency $\omega = \omega_0$ in the band structure. These results are also confirmed by numerical experiments. Our results are only valid for the one-dimensional case. However, we expect some of the ideas may apply to the higher-dimensional case. In higher dimensions, the full operator $\mathcal{C}$ needs to be considered with appropriate energy space for all the vector fields involved. Since the eigenvalues cannot be calculated explicitly, other indirect method has to be used to show that ω_0 is an accumulation point of the eigenvalues and hence lies in the essential spectrum. On the other hand, the Weyl's criterion argument may still work to show that ω_0 is the only

essential spectrum. With these, one may establish the completeness of eigenfunctions and explain the similar phenomenon of pile up of dispersion curves near the singular frequency $\omega = \omega_0$ in the band structure (indicated in the numerical example in [5]).

Acknowledgements
Many people have contributed to this work through discussions. These include David Dobson, Michael Weinstein, Junshan Lin, Stephen Shipman, Braxton Osting, and Eric Bonnetier. This project was initiated at Hong Kong University of Science and Technology where FS was a visiting professor in January 2019. He thanks his hosts for the hospitality during the productive stay. The research of FS is funded in part by the National Science Foundation under DMS 1440471. The research of HZ is partially funded by Hong Kong RGC Grant GRF 16306318 and GRF 16304517.

Author details
[1]School of Mathematics, University of Minnesota, Minneapolis, MN 55455, USA, [2]Department of Mathematics, The Hong Kong University of Science and Technology, Clear Water Bay, Kowloon, SAR, China.

Received: 28 October 2019 Accepted: 12 June 2020 Published online: 6 July 2020

References

1. Courant, R., Hilbert, D.: Methods of Mathematical Physics, vol. 1, pp. 358–361. Interscience Publishers, Geneva (1953)
2. El-Kady, I., Sigalas, M., Biswas, R., Ho, K., Soukoulis, C.: Metallic photonic crystals at optical wavelengths. Phys. Rev. B **62**, 15299–15302 (2000)
3. Hao, X., Sun, J., Zettl, A.: The spectrum of differential operators and square integrable soutions. J. Funct. Anal. **262**, 1630–1644 (2012)
4. Hislop, P., Sigal, I.: Introduction to Spectral Theory with Application to Schrödinger's Equation. Springer, Berlin (1996)
5. Raman, A., Fan, S.: Photonic band structure of dispersive metamaterials formulated as a Hermitian eigenvalue problem. Phys. Rev. Lett. **104**, 087401 (2010)
6. Reed, M., Simon, B.: Functional Analysis, Volume I: Methods of Modern Mathematical Physics, Revised and enlarged edition, Academic Press, INC., Cambridge (1980)
7. Scalora, M., Bloemer, M., Pethel, A., Dowling, J., Bowden, C., Manka, A.: Transparent, metallo–dielectric, one-dimensional, photonic band-gap structures. J. Appl. Phys. **83**, 2377–2383 (1998)
8. Toader, O., John, S.: Photonic band gap enhancement in frequency-dependent dielectrics. Phys. Rev. E **70**, 046605 (2004)
9. Wu, C., Chung, Y., Syu, B., Yang, T.: Band gap extension in a one-dimensional ternary metal–dielectric photonic crystal. Prog. Electromagn. Res. PIER **102**, 81–93 (2010)
10. Yee, K.: Numerical solution of initial boundary value problems involving Maxwell's equations in isotropic media. IEEE Trans. Antennas Propag. **14**, 302–307 (1966)

Publisher's Note